

J. KASPARIAN<sup>✉</sup>  
J. SOLLE  
M. RICHARD  
J.-P. WOLF

## Ray-tracing simulation of ionization-free filamentation

LASIM, UMR CNRS 5579, Université Claude Bernard Lyon 1, 43 bd du 11 Novembre 1918, 69622 Villeurbanne Cedex, France

Received: 25 August 2004/Revised version: 4 October 2004  
Published online: 4 November 2004 • © Springer-Verlag 2004

**ABSTRACT** A new ray-tracing scheme is proposed to simulate the non-linear propagation of ultra-short pulses. The results are in good agreement with experimental data and numerical solving of the non-linear Schrödinger equation in both the self-focusing and the filamentation regions. In particular, they indicate a major contribution of the ‘photon bath’ in the self-guided propagation of ultra-short pulses. The model suggests that a pure-Kerr self-guiding mode can allow filamentation without ionization.

PACS 42.65.Jx; 42.15.Dp

When they propagate in air, high-power, ultra-short (femtosecond) laser pulses can undergo a self-guided mode known as filamentation [1]. This regime is initiated above a critical power  $P_{\text{cr}} = 3.37\lambda^2/(8\pi n_2)$  ( $P_{\text{cr}} = 3$  GW in air at 800 nm, with  $n_2 = 3 \times 10^{-23}$  m<sup>2</sup>/W), when Kerr-lens self-focusing overcomes diffraction. It results in one or several filaments of about 100 μm in diameter that propagate over distances much longer than the Rayleigh length, up to the kilometre range [2]. Filaments can be characterized as transversely localized structures in the beam, with a very high, quasi-constant, intensity [3, 4], which allows efficient self-phase modulation and generation of a broadband white-light continuum spanning from the UV [5] to the mid IR [6]. Ionization of the air within the filament is generally considered to contribute to its self-guiding by providing a stabilizing saturation to counterbalance the Kerr effect and prevent the beam from collapsing. Ionization has been observed experimentally [7–10] and accurately modelled theoretically [11, 12], both in the low-power (single-filamentation) and high-power (multiple-filamentation) regimes. However, its universal con-

tribution to filamentation has recently been challenged by several groups, and ionization-free filamentation regimes have been observed, e.g. in air at very long distances with strongly chirped pulses [13] and in water [14]. Moreover, a new propagation regime known as X-waves has recently been demonstrated in both LBO crystals [15] and water [16].

The properties of the filaments open exciting perspectives for applications [17] such as white-light lidar (light detection and ranging) [18, 19] and laser lightning control [20, 21]. Potential applications in turn stimulate the need for a better characterization of the filament propagation, as well as efficient modelling over atmospheric scales, i.e. in the km range. In particular, the filaments’ onset and length are key parameters for spectroscopic measurements of atmospheric compounds and for depositing the desired intensities on remote targets. However, most numerical simulations [22–25] require either unreasonable computing times to get an insight into the km-range propagation and/or large beam apertures, or require particular conditions such as radial symmetry or Gaussian beam envelopes.

Hence, there is a clear need for a complementary approach towards faster models for the simulation of the propagation of ultra-short laser pulses in air. Such a model should be able to simulate the propagation over kilometres within short computing times of typically several minutes, compatible with real-time analysis of e.g. lidar measurements. Due to the complexity of the underlying physics, which prevents an exact calculation under these conditions, phenomenological models have to be developed. Shortly after self-focusing was discovered [26, 27], several groups [28–32] studied this phenomenon using the geometrical optics approximation. This approach allowed them to analytically reproduce the wavefront curvature and the beam collapse at the non-linear focus. However, geometrical optics intrinsically yields a divergence of the intensity value at the non-linear focus as well as at local hot spots within the beam profile (e.g. in the case of multiple filamentation). Therefore, this approach is not suitable to model subsequent filamentation. This limitation can be overcome by explicitly tracing individual rays, as was recently applied successfully to several non-linear propagation problems such as black holes or mirages [32]. However, contrary to these systems where the refractive-index field is independent of the incident light, Kerr-lens self-focusing locally couples neighbouring rays within the beam, through the intensity-dependent (Kerr) index of refraction ( $n = n_0 + n_2 I$ ). Therefore, rays cannot be propagated independently, but must instead be considered simultaneously.

In this letter, we propose a three-dimensional ray-tracing scheme suit-

✉ Fax: +33-47244-5871, E-mail: jkaspari@lasim.univ-lyon1.fr

able for describing some features of the propagation of high-power laser pulses over long distances. An oversampling of rays within the cells where the local intensity is computed prevents the algorithm from diverging when individual rays cross each other, allowing for simulations beyond the non-linear focus. Therefore, this scheme is suited to describe not only the self-focusing, but also the filamentation region. However, compared with models solving the non-linear Schrödinger equation (NLSE), ray tracing is intrinsically limited to a loose resolution because transverse averaging must occur over cross sections much larger than the laser wavelength. The resolution is therefore of the same order of magnitude as the filament diameter. Therefore, our model does not provide a detailed insight into the physical mechanisms within the filaments themselves, as NLSE-based models do. Instead, it aims at providing a phenomenological, macroscopic description of some features of non-linear, long-distance propagation of laser pulses, such as the position of the filamentation onset or the filamentation length, which are required for applications. In that regard, results of ray tracing are shown to agree well with more accurate, wave-propagation models solving the non-linear Schrödinger equation.

Moreover, since diffraction is neglected in geometrical optics, our model is restricted to regimes where the Kerr effect dominates diffraction, i.e. for powers exceeding several critical powers. Besides providing a fast calculation without symmetry assumptions, ray tracing provides a direct representation of the ray propagation, yielding an intuitive picture of the propagation and self-focusing processes.

The simulations are conducted as follows. The initial beam cross section is sampled transversally into typically  $120 \times 120$  cells, corresponding to a resolution of less than  $100 \mu\text{m}$  for a cm-scale beam (e.g.  $50 \mu\text{m}$  in the presented simulations). 100 rays, evenly spread transversally, are launched from each cell, each one bearing a power determined by its position in the initial beam profile. The initial spacing between the rays is one-tenth of the spatial resolution, i.e.  $5 \mu\text{m}$  in the presented simulations. At each iteration, the inten-

sity profile is computed by summing the power of all rays contained in each cell, and used to compute the local non-linear change of the refractive index  $\Delta n(r) = n_2 I(r)$ . This profile determination, relying on cells containing many filaments each, prevents the calculation from diverging when two neighbouring rays cross each other, as is the case in conventional ray-tracing schemes [30, 31] where the local intensity changes are derived from the distance between adjacent rays. Therefore, it allows us to use our algorithm beyond the onset of local foci, as well as beyond the non-linear focus, i.e. in the filamentation region.

Once the refractive-index profile is determined, each ray is propagated over the iteration distance  $dz$  (typically in the mm to cm range) in the obtained refractive-index gradients. The trajectory of each ray within the iteration is calculated analytically using the classical Fresnel (mirage) formula. The arrival position of each ray is used as the input to calculate the initial intensity profile used for the next iteration. As usual in geometrical optics, diffraction is not taken into account, and the pulse is averaged temporally, assuming a constant pulse duration. Multiphoton ionization is also neglected in our simulations, as well as group-velocity dispersion. To permit comparisons with previously published calculations and experiments, all the simulations presented here have been performed using initially Gaussian beam profiles, with the beam diameters defined at  $1/e$ . Note

that the beam profile is not constrained to stay Gaussian along the propagation, and arbitrary initial profiles can be implemented as well. Besides increasing the versatility of the model, the unconstrained beam profile prevents the beam from collapsing at a non-linear focus, as is the case in many other ray-tracing models [28–32].

We first checked our model by computing the position of the onset of filamentation. This distance is one of the most critical parameters for applications, e.g. for the delivery of high powers at remote locations [33]. In our calculation, we defined it as the first maximum of the on-axis intensity along the propagation. Figure 1 shows this non-linear focusing distance as a function of the power, for parameters typical of the Teramobile system [34]: 330-mJ pulses at 800 nm, with an initial Gaussian beam of 1.5-cm radius at  $1/e$ . The power is varied by changing the pulse duration. Our results compare well with the widely used empirical Marburger formula [35]. The discrepancy is less than 20% for input powers above  $10P_{\text{cr}}$ , corresponding to powers at which the Kerr effect dominates diffraction, which is neglected in geometrical optics. This agreement shows the validity of the ray-tracing technique in the self-focusing region.

However, our ray-tracing scheme does not only provide a fast calculation of the filament onset location. It also offers an intuitive picture of the self-focusing process, by displaying rays

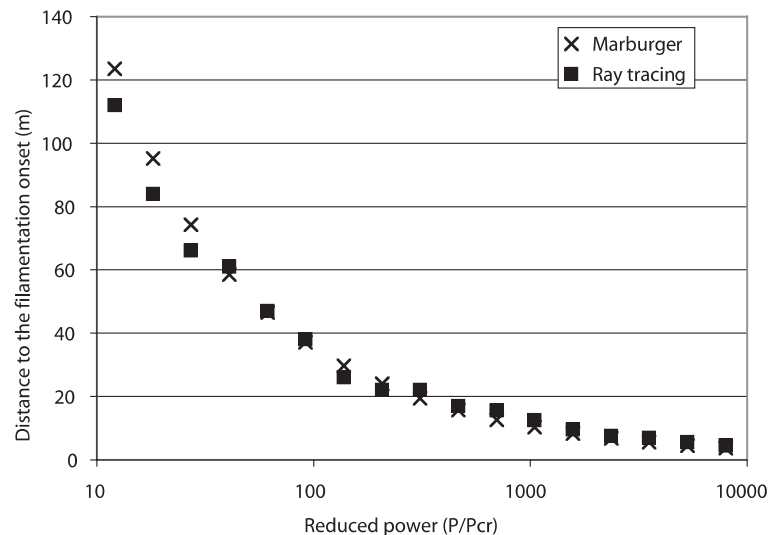


FIGURE 1 Propagation distance before the filamentation onset in the case of single filamentation

along their propagation. This can be more illustrative than displaying e.g. beam diameters, whose meaning can become ambiguous as the beam profile evolves during the propagation. Rays may even cross each other. For example, experiments as well as numerical simulations [36] with an initially Gaussian beam profile provide evidence for the formation of an intense ring during the early stages of propagation. Filaments later arise from the outer band of this ring before merging into the centre of the beam. As shown in Fig. 2, ray tracing suggests a physical picture to understand this effect. Due to the non-uniform intensity profile (and hence refractive-index gradient), some rays, which are located in a region of higher gradient, are focused more strongly than rays located in more homogeneous regions (see arrow 1 in Fig. 2) in the centre or on the edge of the beam profile. Therefore, the intensity decreases in the external vicinity of these focused rays, which further lowers the local intensity and can yield a local refractive-index gradient directed towards the outer region of the beam. This outward-directed gradient locally defocuses the rays propagating in this region (see arrow 2 in Fig. 2), until they reach a region of stronger intensity and positive gradient, which will focus them again (see arrow 3 in Fig. 2). This transient defocusing effect, due to the cross-(de)focusing of nearby

regions of the same beam, increases the non-linear self-focusing distance of the outer regions of the beam, leading to longer filaments. This description can be compared with the moving-focus model [37], except that we consider radially concentric geometrical slices of the beam profile instead of temporal slices of the laser pulse. However, while the temporal slices are independent, except for the retarded Kerr effect and ionization (the latter being negligible outside of the filaments themselves), the cross-defocusing process couples the geometrical slices. This process prolongs the life of the filaments, and might in some conditions allow self-focusing to occur beyond the geometrical focus, as often observed but not explained by the standard moving-focus model [38]. This extension of the moving-focus model may widely extend its applicability range for practical use in long-distance applications, as the extended moving focus of Kosareva et al. [39] does from the theoretical point of view.

While ray tracing had already been shown to yield good results in the self-focusing region, where the Kerr effect is clearly dominating, long-distance simulations require us to be able to reproduce the filament propagation as well. Here, models based on wave propagation require extensive calculations associated with lengthy computation times. In par-

ticular, multiphoton ionization has to be taken into account, not only because it is one of the main physical mechanisms at play in filamentation, but also because it is required to avoid the collapse of the beam, which is known to occur when the NLSE is integrated in the paraxial approximation [40].

However, as shown in Fig. 3, our ray-tracing simulations without ionization reproduce well recent propagation experiments comparing free propagation with filaments perturbed by the interaction with an obscurant [41]. We used the same parameters as in the experiment, namely a slightly focused ( $f = 5$  m) beam at 800 nm, with 7-mJ pulse energy and a pulse duration of 140 fs. The initial beam radius was 1.5 mm at  $1/e$ . Obscurants up to 400  $\mu\text{m}$  have been investigated in the simulations. Our simulations reproduce well the experimental results, in terms of the filamentation start and end, and of the evolution of the fluence. They also agree semi-quantitatively with the results of extensive numerical simulations based on the NLSE and taking into account the effects of diffraction, stimulated Raman scattering, plasma generation and the interaction of light with the plasma [42]. In particular, the fluence values and the refocusing along the propagation, as well as the filamentation length of 3–4 m, agree very well. Here, the filament end is defined as the strong fluence decrease down to values comparable to the initial one.

The survival of filaments in spite of large obscurants [41] shows that their re-feeding by the ‘photon bath’ [23, 24], focused by the Kerr effect, critically contributes to filamentation, as opposed to a local balance between the Kerr effect and the plasma.

Moreover, it is well known that under the usual propagation conditions in air, ionization balances the Kerr effect and allows the self-guiding of the filaments. However, such a regularizing contribution is mathematically required to avoid collapse of the NLSE only when it is solved in the frame of the paraxial approximation [40]. Since our ray-tracing calculations do not use the paraxial approximation, there is no reason to expect them to yield a beam collapse. This pure-Kerr, collapse-free propagation mode might help understand the recent observation

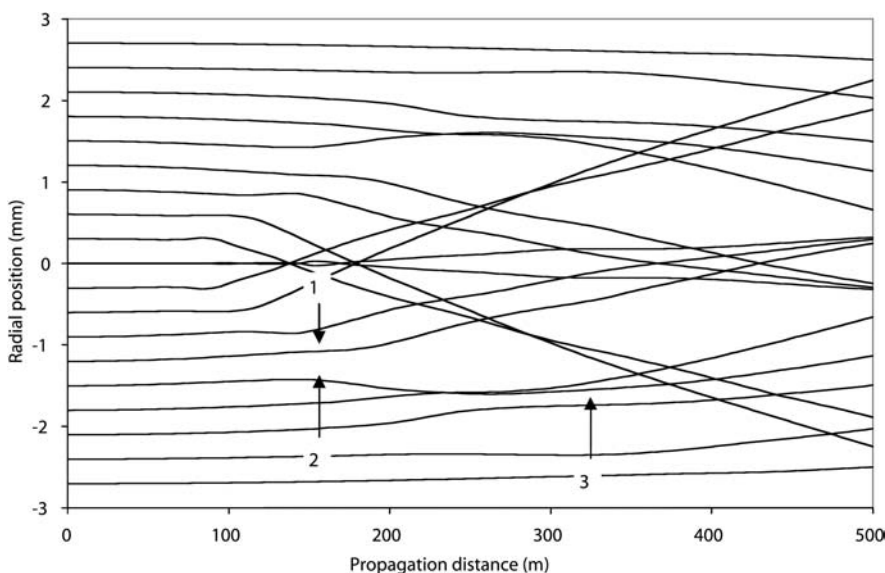


**FIGURE 2** Ray-tracing simulation of the propagation of a laser pulse (7 mJ, 140 fs, 1.5-mm radius at  $1/e$ ). For clarity, only 20 evenly spaced rays in the transverse plane are displayed, corresponding to 60-times downsampling. Cross-(de)focusing of neighbouring rays is clearly visible, as marked by the arrows (see text for details)

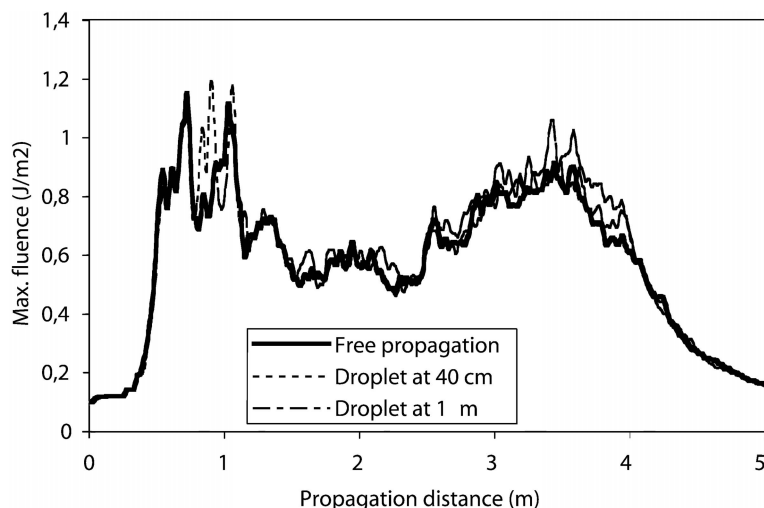


**FIGURE 3** Ray-tracing simulation of the maximum fluence across the beam cross section for both free propagation and propagation perturbed by a spherical obstacle

of filamentation at distances in the km range [2, 43], which was interpreted as due to an ionization-free regime [43]. This result is also similar to that of Dubietis et al. [14], which was obtained with a simplified propagation model.

Moreover, ray tracing suggests an intuitive description for this ionization-free self-guided propagation regime. Since the different spatial regions of the beam do not self-focus at the same distance, rays can be refocused by the ‘photon bath’ after they have crossed their non-linear focus, as shown in Fig. 4. This suggests a new mode of pure-Kerr self-guiding of ultra-short laser pulses, governed by macroscopic cross-folding

of spatial beam regions. The reduced contribution of small-scale guiding is further supported by the small effect of obstacles located on the beam axis.

As a conclusion, ray-tracing simulations of long-range propagation of ultra-short laser pulses in air, although neglecting ionization and considering the Kerr effect as the only non-linear process at play, can reproduce some macroscopic features relevant for atmospheric applications, such as the filament onset and length, or the fluence evolution. While this technique has a limited resolution and does not describe the filamentation physics at the microscopic scale, it fits with the corresponding re-

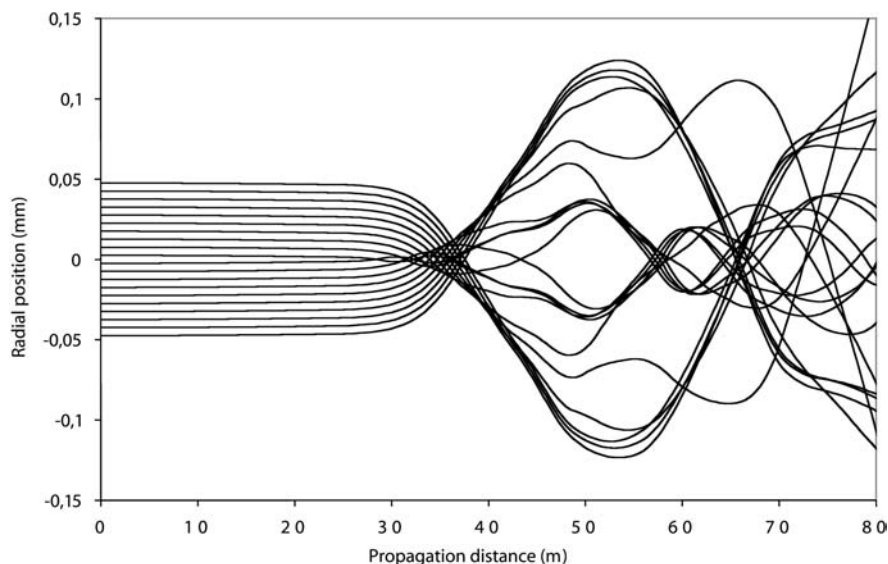


**FIGURE 4** Kerr-only refocusing of rays near to the centre of a 330-mJ, 900-fs beam of 1.5-cm radius at  $1/e$ . For clarity, the graph displays a close-up of the 20 most central rays, within the much wider beam profile

sults of wave-propagation models, although with strongly reduced computing times and computer requirements, as well as with much flexibility in setting the initial conditions, as is suitable for field use in view of applications such as lidar pollution monitoring and lightning control.

Besides, ray tracing provides an intuitive picture of the self-focusing and self-guiding processes. In this regard, we suggest an interpretation of both the formation of filaments on a ring in high-power beams as a cross-defocusing effect among neighbouring regions of the beam and ionization-free filamentation in terms of large-scale cross-refocusing of different beam slices.

## REFERENCES

- 1 A. Braun, G. Korn, X. Liu, D. Du, J. Squier, G. Mourou: *Opt. Lett.* **20**, 73 (1995)
- 2 M. Rodriguez, R. Bourayou, G. Méjean, J. Kasparian, J. Yu, E. Salmon, A. Scholz, B. Stecklum, J. Eislöffel, U. Laux, A.P. Hatzes, R. Sauerbrey, L. Wöste, J.-P. Wolf: *Phys. Rev. E* **69**, 036607 (2004)
- 3 J. Kasparian, R. Sauerbrey, S.L. Chin: *Appl. Phys. B* **71**, 877 (2000)
- 4 A. Becker, N. Aközbe, K. Vijayalakshmi, E. Oral, C.M. Bowden, S.L. Chin: *Appl. Phys. B* **73**, 287 (2001)
- 5 N. Aközbe, A. Iwasaki, A. Becker, M. Scallora, S.L. Chin, C.M. Bowden: *Phys. Rev. Lett.* **89**, 143901 (2002)
- 6 J. Kasparian, R. Sauerbrey, D. Mondelain, S. Niedermeier, J. Yu, J.-P. Wolf, Y.-B. André, M. Franco, B. Prade, A. Mysyrowicz, S. Tzortzakis, M. Rodriguez, H. Wille, L. Wöste: *Opt. Lett.* **25**, 1397 (2000)
- 7 H. Schillinger, R. Sauerbrey: *Appl. Phys. B* **68**, 753 (1999)
- 8 S. Tzortzakis, B. Prade, M. Franco, A. Mysyrowicz: *Opt. Commun.* **181**, 123 (2000)
- 9 B. La Fontaine, F. Vidal, Z. Jiang, C.Y. Chien, D. Comtois, A. Desparois, T.W. Johnston, J.-C. Kieffer, H. Pépin, H.P. Mercure: *Phys. Plasmas* **6**, 1615 (1999)
- 10 A. Talebpour, A. Abdel-Fattah, S.L. Chin: *Opt. Commun.* **183**, 479 (2000)
- 11 J. Kasparian, R. Sauerbrey, S.L. Chin: *Appl. Phys. B* **71**, 877 (2000)
- 12 A. Talebpour, J. Yang, S.L. Chin: *Opt. Commun.* **163**, 29 (1999)
- 13 G. Méchain, A. Couairon, Y.-B. André, C. D’Amico, M. Franco, B. Prade, S. Tzortzakis, A. Mysyrowicz, R. Sauerbrey: *Appl. Phys. B* **79**, 379 (2004)
- 14 A. Dubietis, E. Gaizauskas, G. Tamosauskas, P.D. Trapani: *Phys. Rev. Lett.* **92**, 253903 (2004)
- 15 C. Conti, S. Trillo, P. Di Trapani, G. Valiulis, A. Piskarskas, O. Jedrkiewicz, J. Trull: *Phys. Rev. Lett.* **90**, 170406 (2003)
- 16 M. Kolesik, E.M. Wright, J.V. Moloney: *Phys. Rev. Lett.* **92**, 253901 (2004)
- 17 J. Kasparian, M. Rodriguez, G. Méjean, J. Yu, E. Salmon, H. Wille, R. Bourayou, S. Frey,

- Y.-B. André, A. Mysyrowicz, R. Sauerbrey, J.-P. Wolf, L. Wöste: *Science* **301**, 61 (2003)
- 18 P. Rairoux, H. Schillinger, S. Niedermeier, M. Rodriguez, F. Ronneberger, R. Sauerbrey, B. Stein, D. Waite, C. Wedekind, H. Wille, L. Wöste: *Appl. Phys. B* **71**, 573 (2000)
- 19 G. Méjean, J. Kasparian, E. Salmon, J. Yu, J.-P. Wolf, R. Bourayou, R. Sauerbrey, M. Rodriguez, L. Wöste, H. Lehmann, B. Stecklum, U. Laux, J. Eislöffel, A. Scholz, A.P. Hatzes: *Appl. Phys. B* **77**, 357 (2003)
- 20 B. La Fontaine, D. Comptois, C.Y. Chien, A. Desparois, F. Gérin, G. Jarry, T.W. Johnston, J.C. Kieffer, F. Martin, R. Mawassi, H. Pépin, F.A.M. Rizk, F. Vidal, C. Potvin, P. Couture, H.P. Mercure: *J. Appl. Phys.* **88**, 610 (2000)
- 21 M. Rodriguez, R. Sauerbrey, H. Wille, L. Wöste, T. Fujii, Y.-B. André, A. Mysyrowicz, L. Klingbeil, K. Rethmeier, W. Kalkner, J. Kasparian, E. Salmon, J. Yu, J.-P. Wolf: *Opt. Lett.* **27**, 772 (2002)
- 22 A. Couairon, L. Bergé: *Phys. Rev. Lett.* **88**, 135003 (2002)
- 23 M. Mlejnek, E.M. Wright, J.V. Moloney: *Opt. Express* **4**, 223 (1999)
- 24 M. Mlejnek, M. Kolesik, J.V. Moloney, E.M. Wright: *Phys. Rev. Lett.* **83**, 2938 (1999)
- 25 P. Sprangle, J.R. Peñano, B. Hafizi: *Phys. Rev. E* **66**, 046418 (2002)
- 26 G.A. Askar'yan: *Sov. Phys. J. Exp. Theor. Phys.* **15**, 1088 (1962)
- 27 R.Y. Chiao, E. Garmire, C.H. Townes: *Phys. Rev. Lett.* **13**, 479 (1964)
- 28 D. Censor: *Phys. Rev. A* **16**, 1973 (1977)
- 29 M.N.Y. Anwar, R.D. Small: *J. Opt. Soc. Am.* **71**, 124 (1981)
- 30 I. Dajani, G. DiPeso, E.C. Morse, R. Ziolkowski: *Phys. Rev. A* **41**, 3740 (1990)
- 31 M. Sonnenschein, D. Censor: *J. Opt. Soc. Am.* **15**, 1335 (1998)
- 32 T.R. Satoh: *J. Winter Sch. Comput. Graphics* **11**, 402 (2003)
- 33 K. Stelmaszczyk, P. Rohwetter, G. Méjean, J. Yu, E. Salmon, J. Kasparian, R. Ackermann, J.-P. Wolf, L. Wöste: "Long-distance remote laser-induced breakdown spectroscopy using filamentation in air", to be published in *Appl. Phys. Lett.* (2004)
- 34 H. Wille, M. Rodriguez, J. Kasparian, D. Mondelain, J. Yu, A. Mysyrowicz, R. Sauerbrey, J.-P. Wolf, L. Wöste: *Eur. Phys. J. – Appl. Phys.* **20**, 183 (2002)
- 35 J.H. Marburger, E.L. Dawes: *Phys. Rev. Lett.* **21**, 556 (1968). Note that the radius considered in the classical writing of Marburger's formula is the half width at  $e^{-1/2}$ , not the usual  $1/e$  or  $1/e^2$  definitions
- 36 L. Bergé, S. Skupin, F. Lederer, G. Mejean, J. Yu, J. Kasparian, E. Salmon, J.-P. Wolf, M. Rodriguez, L. Wöste, R. Bourayou, R. Sauerbrey: *Phys. Rev. Lett.* **92**, 225002 (2004)
- 37 A. Brodeur, C.Y. Chien, F.A. Ilkov, S.L. Chin, O.G. Kosareva, V.P. Kandidov: *Opt. Lett.* **22**, 304 (1997)
- 38 H.R. Lange, G. Grillon, J.-F. Ripoche, M.A. Franco, B. Lamouroux, B.S. Prade, A. Mysyrowicz, E.T.J. Nibbering, A. Chiron: *Opt. Lett.* **23**, 120 (1998)
- 39 O.G. Kosareva, V.P. Kandidov, A. Brodeur, S.L. Chin: *J. Nonlinear Opt. Phys. Mater.* **6**, 485 (1997)
- 40 G. Fibich, G. Papanicolaou: *SIAM J. Appl. Math.* **60**, 183 (1999)
- 41 F. Courvoisier, V. Boutou, J. Kasparian, E. Salmon, G. Méjean, J. Yu, J.-P. Wolf: *Appl. Phys. Lett.* **83**, 213 (2003)
- 42 M. Kolesik, J.V. Moloney: *Opt. Lett.* **29**, 590 (2004)
- 43 G. Méchain, A. Couairon, Y.-B. André, C. D'Amico, M. Franco, B. Prade, S. Tzortzakis, A. Mysyrowicz, R. Sauerbrey: *Appl. Phys. B* **79**, 379 (2004)